

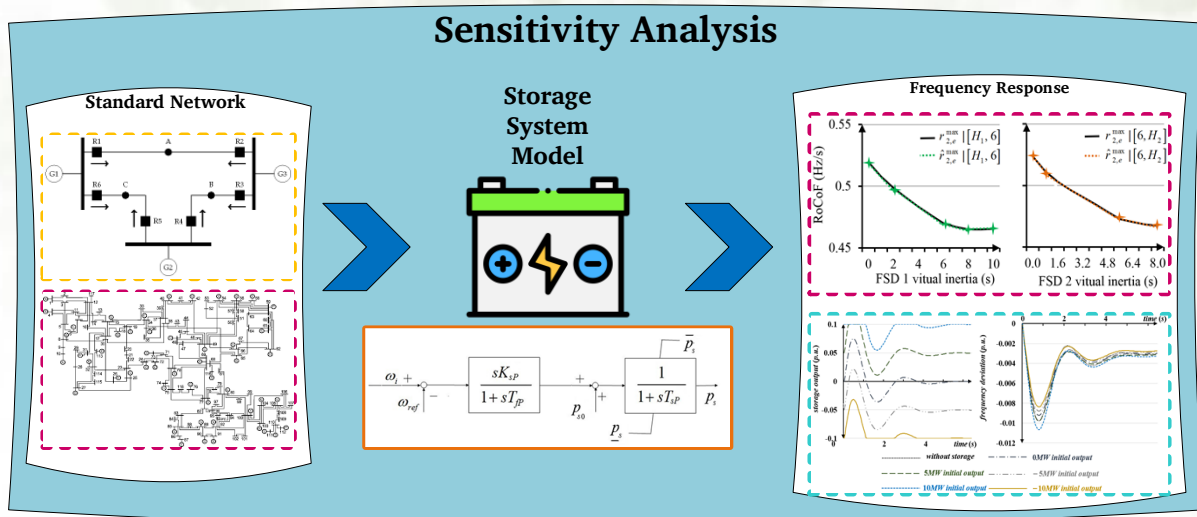
Sensitivity Analysis of the Problem of Contribution of Energy Storage Devices to Providing Inertia for the Primary Frequency Response

Moaiaad Mohseni, Alireza Niknam Kumleh, Rezvan Keshavarzpour

Highlight

- ❖ Providing an inertial response for ESS with fast response capability
- ❖ Investigating the effect of inertial response in establishing frequency response and network behavior after sudden events
- ❖ Considering the new model of the problem and applying the novel algorithm for this problem

Graphical Abstract



Use your device to scan and read the article online



Citation

M. Mohseni, A. Niknam Kumleh, and R. Keshavarzpour, "Sensitivity Analysis of the Problem of Contribution of Energy Storage Devices to Providing Inertia for the Primary Frequency Response," *Journal of Green Energy Research and Innovation*, vol. 1, no. 3, pp. 30-48, 2024.

 <https://doi.org/10.61186/jgeri.1.3.30>

© Author 



Sensitivity Analysis of the Problem of Contribution of Energy Storage Devices to Providing Inertia for the Primary Frequency Response

Moaiad Mohseni ^{1*}, Alireza Niknam Kumleh ², Rezvan Keshavarzpour ³

¹ Khuzestan Regional Electric Company, Ahvaz, Iran.

² Faculty of Electrical Engineering, Amirkabir University of Technology (Tehran polytechnic), Tehran, Iran.

³ National Iranian South Oil Company (NISOC), Ahvaz, Iran.

* Corresponding Author: moaiadmohsenii@gmail.com

ARTICLE INFO

Keywords:

Primary frequency, response, Energy storage, Virtual inertia, Sensitivity analysis.

Article history:

Received: 11 March 2024;
Revised: 12 April 2024;
Accepted: 29 April 2024;

Article type:

Research Article

ABSTRACT

Today, with the expansion of low-inertia (such as wind power plants) and non-inertia (such as photovoltaic power plants) technologies, the amount of network inertia and power related to the primary frequency response has decreased significantly. As a result, in the event of disturbances, the frequency changes with a relatively higher slope and it may violate its permissible range. To solve this problem, several methods have been presented so far that create artificial inertia by power electronic converters connected to storage devices or renewable generation. Therefore, the models make the operation of these sources similar to traditional power plants and increase their contribution to the frequency response during storage contribution events. In this paper, the sensitivity analysis of energy storage contribution to providing inertia for the primary frequency response has been carried out. IEEE 3-bus and 118-bus networks are used as test networks. MATLAB software is also adopted for optimization. The results show the impact of each storage parameter on the frequency response and how it is possible to meet the frequency response limitations of the network by managing the storage devices.

1. Introduction

Distributed generations (DGs) such as photovoltaics (PVs) and wind turbines (WTs) have expanded in recent years in power systems and some cases have replaced fossil units [1]. Renewable energy sources (RESs) are highly dependent on climate changes and high fluctuations in their output power are observed. To deal with and eliminate these fluctuations, energy storage systems (ESS) are usually used, which have many advantages such as high response speed, stable power transmission, and no dependence on climatic conditions. One of the issues regarding ESS is their optimal placement in the network, determining their optimal size, and managing their charging status in the network. Adding storage devices to the network requires an initial investment cost, but with its optimal design and management, the total costs of network operation can be reduced. Many studies have been presented in the field of optimal design of ESS. Reference [2] reviewed these methods and their design criteria. Reference [3] provided a review of battery

technology for energy storage. ABB company has designed a storage system and a special converter for it, which provides inertial response in power systems with high reliability. The speed of this system is very high and its ability to reduce frequency deviations has been well proven [3]. In reference [4], storage batteries were used to provide the primary frequency response. In fact, the combined storage system including a battery and a supercapacitor was used to provide the primary frequency response of an isolated microgrid. The principles of providing primary frequency response using storage devices are based on the management and planning of coordinated charging of storage devices. Reference [5] suggested the implementation of a market for frequency response reserve (FRR) in the future grid, specifically targeting generators and load resources equipped with under-frequency relays. The purpose of [6] was to investigate the notion of orientational smoothing in conjunction with the frequency management of deloaded photovoltaic (PV) systems to enhance self-balancing, decrease reliance on battery energy storage systems (BESS), and guarantee a consistently higher availability of regulatory reserves. Study [7] optimized temporary main frequency control parameters during rotor speed recovery using an analytically determined technique to limit secondary frequency deviation induced by DFIG inertial control. Optimized parameters included termination time and active power. Literature [8] focused on the current research trend that aims to increase the participation of wind turbine generators in rapidly regulating the grid frequency (inertia emulation), in addition to conventional power system alternators. Reference [9] presented an adaptive primary frequency support technique for clusters of electric vehicles (EVs) that are limited by the operation region specified by their charging behavior. In reference [10], a DC microgrid was investigated from the point of view of secondary frequency response. This microgrid included RESs and the use of energy storage improved the operation of the microgrid. Energy storage is one of the important components of microgrids that reduce the fluctuations of DGs and improve the operating conditions of the grid both in islanded and grid-connected conditions. In reference [11], integration of ESS units was adopted to provide the secondary frequency response of power systems. In the future, small storage units will be integrated to create a frequency response control service. The method of load frequency control was described in [12] using ESS. In literature [13], the tertiary control of a set of microgrids was presented. In that study, voltage, and frequency control were presented to restore these parameters to their desired nominal value in a set of islanded microgrids. This method is activated when the existing methods for controlling energy storage and generators do not work successfully. This method performs well as a strong support in networks containing a high level of DGs. In reference [14] a storage battery was used to control the voltage and frequency of microgrids. In that study, storage devices with high response speed were incorporated. The results showed that voltage and frequency were able to follow their reference signals suitably. A variety of adaptive control methods for WTs have also been provided, among which the pitch angle control and the rotor speed control have been provided. The results prove that the adaptive control method provides considerably better results than other frequency control methods. From the point of view of the rate of

change of frequency (RoCoF), frequency drop, and reduction of frequency deviation in steady state have been provided. The stepping method of inertial control can reduce the RoCoF, but it leads to a secondary frequency drop [15]. The traditional networks contain a high capacity of synchronous generators (in the form of hydropower, thermal, gas, coal, combined cycle, or nuclear) with high inertia. The high inertia prevents severe frequency deviations in the case of events. Therefore, in the past, the behavior of primary or secondary frequency response was not crucial [16]. Hydroelectric, nuclear, and fossil fuel-based units are naturally effective in providing primary frequency response in two ways. First, due to the high mechanical and kinetic energy of these generation units, these generators provide a high level of inertia response for the grid whenever they are connected to the grid. Second, the inherent characteristic of these units is that they are usually kept connected for a long time, and this leads to a longer persistence of inertia in the network [17]. The emergence of clean energies and their high penetration level in the power system can be considered the main factor of the emergence of frequency response limitations in power system problems. Frequency recovery, the discussion on the frequency stability of the network against disturbances, and the adjustment of the frequency response of the network against sudden incidents of the network are among the priorities of recent research on the operation of power systems. Also, the solutions to increase the penetration level of DGs in the system and the approaches to provide as much inertia as possible are among the most important recent challenges of the frequency response studies of the power system. The effects related to the uncertainty of the behavior of these DGs in the frequency of their power system are technically and economically important [18]. Another economic effect of frequency response limitations in network operation is that the network operator must adjust and plan DGs in such a way that at any moment there are units connected to the network that guarantee sufficient frequency response for a network. New planning of power plant units by considering frequency limitations means adding extra costs of network operation [19]. In reference [20], the effect of energy storage in improving the stability of the frequency response was considered. It was shown that the presence of an ESS device of 1 to 2 MWh next to a 10 MW wind farm can provide the possibility of automatic central control during 29 days of the month. Also, the investigation of the capabilities of ESS in the implementation of automatic central control in the wind research park was considered. Reference [21] reviewed the ESS technology and the progress made in this field. It was mentioned that with the current state of the electricity market, it is difficult for ESS units to compete with traditional electricity generation units. In reference [22] determined the optimal capacity of network storages and optimal control of these systems to provide network frequency improvement. Frequency deviations of power systems, which are usually caused by the fluctuations of grid-connected wind generators, are one of the main factors limiting the penetration of distributed RESs. Reference [23] investigated the effect of frequency response limitations in network operation and in the presence of energy storage. Considering the limitation of the RoCoF in planning the generation of power plants and the use of energy storage can have a great impact on the frequency behavior of the

network. In reference [24], the placement and determination of the optimal size of ESS to control the primary frequency response of an isolated section of the Mexican power grid was presented. The paper showed that the increase in the level of penetration of DGs leads to problems with network frequency. In order to provide the desired frequency response, energy storage batteries were used. In reference [25], the benefits of using energy storage in the market of providing fast frequency response in the national network of England were evaluated. Using equipment with fast response speed can reduce the power imbalance between supply and demand. A real-time strategy for controlling storage devices was presented. Controlling the charge level of energy storage has a significant effect on the life of the storage. In reference [26], ESS was used to prevent under-frequency load shedding. The under-frequency load shedding is one of the temporary measures to prevent the frequency violation at a value lower than the set limit. This action is taken to restore the network to a safe state. By using energy storage and power electronics converters [27], power can be quickly injected into the network, and frequency deviations can be avoided when a power imbalance occurs in the network. In reference [28], lithium-ion batteries were adopted as a tool for fast power transfer in sudden events and stabilization of frequency response. This reference showed how these storage batteries should be installed and utilized in the network. Also, in this research, the charging level of ESS after passing the transient frequency states was optimized. Determining the charge level of energy storage has a significant effect on increasing the life of these equipment. In reference [29], the simultaneous contribution of WTs and ESS to the electricity market to provide frequency response was discussed. In literature [30], the design of the frequency droop controller in hybrid electric vehicles to control the primary frequency response was analyzed. To better understand the primary frequency response control in the presence/absence of ESS, special designs are proposed in this paper and the stability margin of each of these designs is determined. RES and ESS have little or no inertia. Increasing the penetration level of these sources has led to a decrease in network inertia and an increase in the probability of frequency deviation or sudden network collapse. The inertia of the network was not very important in the past, but today, with the penetration of DGs and the change in the dynamic characteristics of the network, the discussion of providing the inertial response and the primary frequency response has received much attention from scholars. One of the most novel approaches to increase network inertia is to utilize the control methods of power electronic converters to show behavior similar to synchronous machines, called virtual inertia, in these sources. This study intends to provide an inertial response for ESS to maintain the frequency stability of the network against the occurrence of sudden events.

The contribution of this paper is to provide an inertial response for ESS with fast response capability. Also, investigating the effect of providing this response in establishing frequency response and network behavior after sudden events is considered among other contributions of this work. Considering the new model of the problem and applying the novel algorithm for this problem are other innovations of current research. Other parts of the paper are structured as follows. In [Section 2](#), the description of the

proposed model is presented. In [Section 3](#), simulations are performed, and a summary of the results is presented in [Section 4](#).

2. Modeling and problem formulation

2.1. Providing the virtual inertia

Inertia response can be created by using fast storage devices because these devices can be charged or discharged at their maximum nominal rate in less than 1 ms. This section of the paper focuses on the primary frequency response, which is dedicated to a period of tens of seconds. Without any specific control strategy, the output level of energy storages (p_s in per-unit or p.u. and P_s in MW) remains at its initial value (i.e., p_{s0} or P_{s0}) after some time (several seconds) after the event. Therefore, fast ESS does not contribute to the transient stability of the network. A method is presented to control the ESS so that they can create virtual inertia H_s in the network. The main idea of this design focuses on controlling the output power of the storage device so that it adjusts its output power based on the local frequency of each of the storage devices. If the local frequency in terms of per-units is f_i and the nominal frequency of the network is $f_B = 60$ Hz, then the corresponding virtual rotation speed is denoted by $\omega_i = 2\pi f_i$ and the nominal rotation speed is expressed by $\omega_B = 2\pi f_B$; therefore, [Equations \(1\) and \(2\)](#) are established.

$$\Delta p_s = p_s - p_{s0} = -2H_s \Delta \dot{\omega}_i \quad (1)$$

$$\Delta p_s \in \left[\underline{p}_s - p_{s0}, \tilde{p}_s - p_{s0} \right] \quad (2)$$

It can be seen that the control signal completely depends on the local frequency. Virtual inertia can be represented by $H_s = \frac{J_s(\omega_B)^2}{2S_B r^2}$ (in seconds) where J_s is in MWs. Therefore, the virtual kinetic energy of the storage device is $E_s = \frac{1}{2} J_s \omega_s^2$ and the virtual mechanical frequency is $\omega_s = \frac{\omega_i \omega_B}{r}$, and r shows the virtual poles of the device. Therefore, the relations can be rewritten as [Equation \(3\)](#):

$$-\Delta P_s = \dot{E}_s = J_s \omega_s \dot{\omega}_s \Leftrightarrow -\Delta p_s = 2H_s \omega_i \dot{\omega}_i \approx 2H_s \dot{\omega}_i \quad (3)$$

Control signals can be measured on the generator side (rotation speed) or the network side (connection point frequency). To achieve real results, storage dynamics, response time, and communication delay are also considered in the simulation. In this paper, ESS is equipped with a dynamic response adjustment controller. The local frequency ω_i can be adjusted using the active power output of the storage control module and the connection point voltage using the reactive power of this module. In this paper, a simplified dynamic model of the storage system is presented, which has two lagging-phase blocks with time constants T_{fP} and T_{sP} . Therefore, the inertial response provided by the module is equal to $K_{sP} = -2H_s \omega_i^2$. This study assumes that the grid power plants are divided into two categories: thermal power plants and gas power plants. Each of these plants has its characteristics and is of special importance from the point of view of dependence on natural gas. It is also assumed that the management of unit commitments will be divided into two parts [\[31\]](#). The first part (upstream) is related to daily planning (or day-ahead

planning) to comply with the restrictions related to daily energy exchange contracts and the general status of power plants in terms of start/shutdown or initialization (binary variables of the problem) should be specified. The second part (downstream) is related to daily operation (same day) in which any uncertainty or fluctuations are answered in the form of adjusting the power generation of power plants (real continuous variables). In this stage, uncertainty has shown itself and usually, the final result of this stage is obtained based on mathematical expectation of probable events. In this paper, uncertainty is considered on the limits of gas supply lines. Also, to understand the effect of natural gas pricing on the problem, separate case studies will be examined. In the following, the mathematical model of the problem is discussed and then the stochastic form of the problem is presented. Figure 2 shows the output power of the storage device and the frequency deviation in different values of the virtual inertia of the storage devices. The higher the virtual inertia, the better the frequency response of the system. Also, higher values of virtual inertia require higher charging and discharging capacity of ESS.

It can be seen in Figure 3 that if the storage capacity is less than 30 MW, by increasing the charging and discharging capacity, the advantages of virtual inertia in improving the primary frequency response will be reduced.

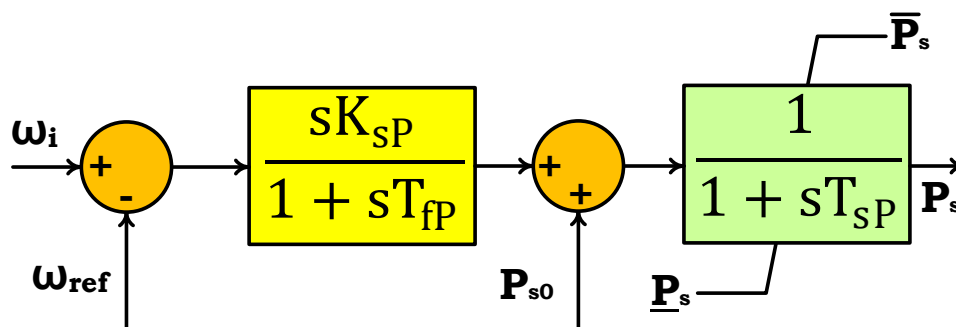


Figure 1. Simplified structure of the grid-connected storage system.

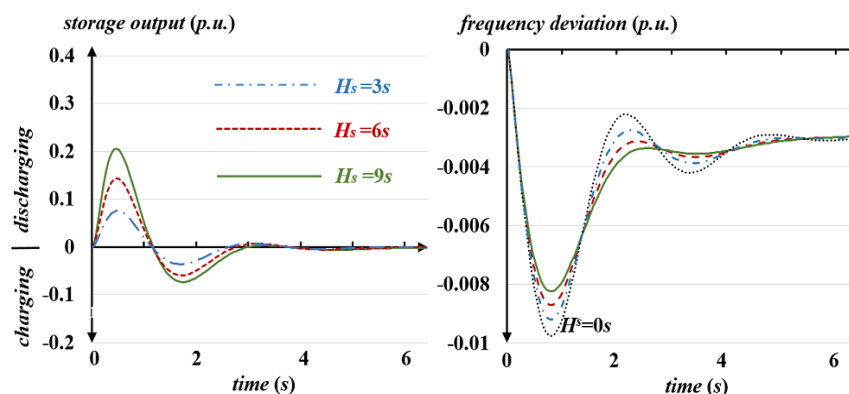


Figure 2. The effect of virtual inertia on the frequency response of the power system considering the dynamics of the storage battery.

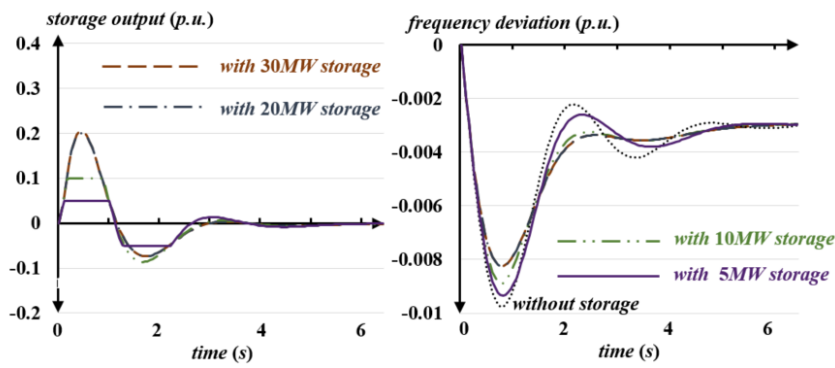


Figure 3. Dynamic simulation by considering the upward charge/discharge limit of storage and dynamics of the storage battery $H_s = 9s$.

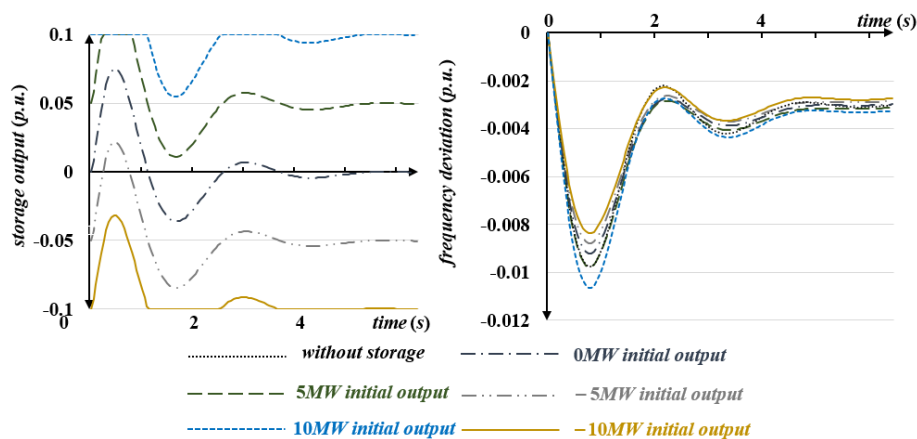


Figure 4. Dynamic simulation with variable initial output of the storage by considering the storage dynamics.

Figure 4 illustrates that the initial output values of the storage devices play a significant role in the behavior of the primary frequency response. The charging state of the storage devices helps to prevent the frequency drop, and the discharge state of the storage devices brings a worse situation in terms of the frequency nadir compared to the state without the use of the storage device. It should also be noted that the storage units with an initial output of -10 MW contribute to the inertial response exactly after the event, but the storage units with an initial output of 10 MW do this only after the frequency drops. These results seem reasonable. Storage devices usually have less free capacity to respond to frequency reduction.

2.2. The problem of minimization of ESS's planning cost

Usually, the generation planning of the power plant is done in 24-hour intervals, and economic load dispatch is carried out every 15 minutes. In fact, after the implementation of the economic load dispatch program every 15 minutes, the necessary measures will be determined to provide transient stability in the next period. To ensure that the frequency or the post-event rate of change occurs within the allowed range, the problem of economic load dispatch is solved.

The purpose of this method is to find the lowest contribution cost of ESS. Under-frequency events are discussed in this paper and the constraints related to the lowest and highest rate of change of frequency are considered in the problem.

2.2.1. Formulation of the storage planning problem

The vector $x = [x_1, x_2, \dots, x_N]^T$ represents the non-negative virtual inertia provided by the storage (decision variables of the optimization problem). The upper and lower limits of these variables are denoted by mathematical symbols $\bar{H} = [\bar{H}_1, \bar{H}_2, \dots, \bar{H}_N]^T$ and $\underline{H} = [\underline{H}_1, \underline{H}_2, \dots, \underline{H}_N]^T$. The problem of economic planning of storage is formulated as Equations (4 - 7):

$$\min_x: c^T x \tag{4}$$

$$s. t: f_{b,e}^{min_b} \tag{5}$$

$$r_{b,e}^{max_b} \tag{6}$$

$$x_n \in \{0, [\underline{H}_n, \bar{H}_n]\}, for \forall n \in N \tag{7}$$

In these equations, $N = \{1, 2, \dots, N\}$ shows the set of storage units, c is the cost of virtual inertia, $f_{b,e}^{min_x}$ is the minimum frequency, and $r_{b,e}^{max_x}$ expresses the rate of change of frequency of each bus $b \in B$ during any given $e \in \varepsilon$ event.

2.3. Iterative solution to problem-solving

Searching in the solution space requires simulating the transient stability of the problem. It seems impractical to provide a comprehensive method for the final results in the real world. To reduce the computational burden, an algorithm for the planning problem is presented in this section. As shown in Figures 5 and 6, linearization can be used to approximate the role of virtual inertia of the storage devices at the minimum frequency of each bus and the highest rate of change of its frequency. The accuracy of the proposed method is optimal. Based on these linearizations, the mixed-integer linear problem is presented and an iterative method will be presented to solve it.

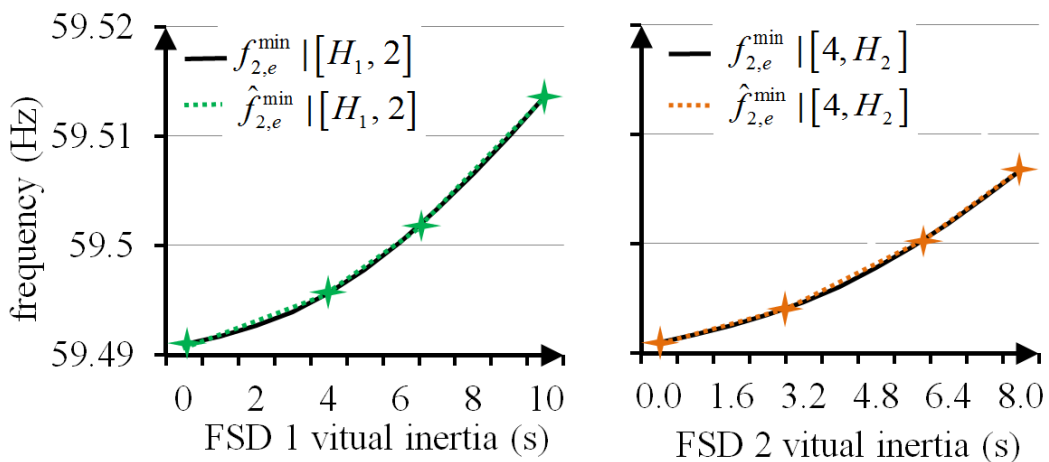


Figure 5. Minimum frequency linearization in a network with two storage devices.

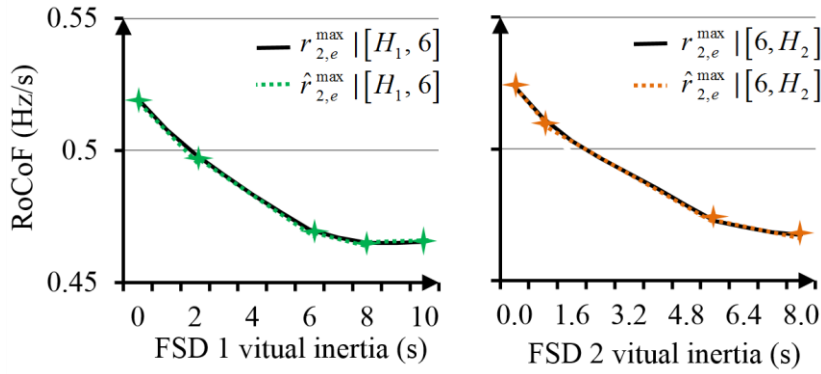


Figure 6. Linearization of the RoCoF in a network with two storage devices.

2.3.1. Formulation of the linearized planning problem

Considering that $\underline{H} \leq x \leq \bar{H}$, each of the solution zones $\{x_n: \underline{H}_n \leq x_n \leq \bar{H}_n\}$ can be divided into \tilde{Z}_n sections. The favorable virtual inertia of the n th storage is shown by a vector $(\tilde{Z}_n + 1) \times 1$, named $h_n = [h_{n,0} = \underline{H}_n, h_{n,1}, \dots, h_{n,\tilde{Z}_n} = \bar{H}_n]^T$. The present settings of the virtual inertia are represented by $H = [h_1, h_2, \dots, h_N]^T$. The only difference between vectors $\hat{H}_{n,z} = [\dots, h_{n,z}, \dots]^T$ and $H = [\dots, h_n, \dots]^T$ is in the virtual inertia settings of the n th storage. Moreover, a vector $\hat{H}_{n,-1} = [\dots, h_{n,-1}, 0, h_{n+1}, \dots]^T$ with $h_{n,-1} = 0$ and $Z_n = \{0, 1, \dots, \tilde{Z}_n\}$ is defined. The metrics under study and their limits are provided as $m \in M = \{f^{\min}, (-r)^{\max}\}$, and $M_b \in \{\mathcal{E}_b, -\tilde{r}_b\}$, respectively. Therefore, the marginal gain of the z th part of virtual inertia's contribution to the n th storage is given as Equation (8). Also, the equivalent index of the rate of change of frequency or the minimum frequency is represented as Equation (9). With a planning

scheme, the value is defined as Equation (10), which shows the value of participated inertia, H , in the range $[h_{n,-1}, h_{n,z}]$. Figure 7 illustrates the definition of parameters.

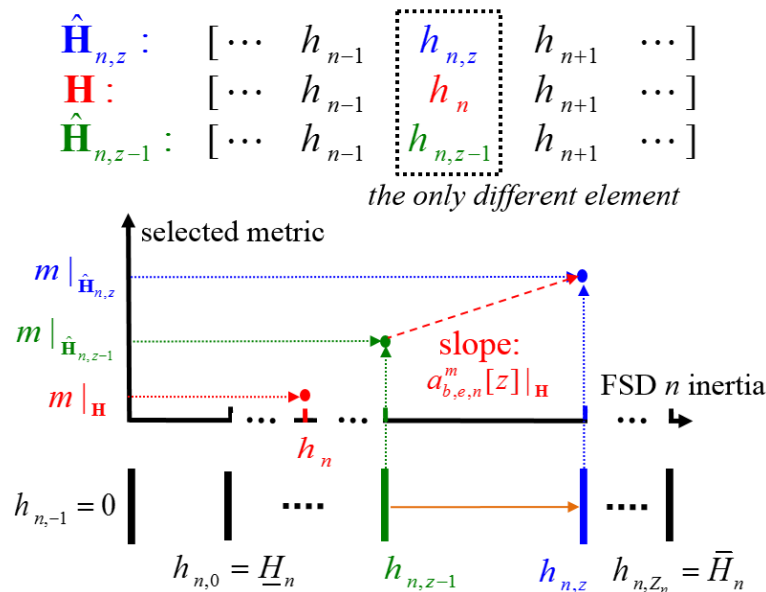


Figure 7. Demonstration of parameters adjustment.

$$\alpha_{b,e,n}^m[z]|_H = \frac{m_{b,e}|_{h_{n,z-1}}}{h_{n,z} - h_{n,z-1}}, \text{ for } z \in Z_n \quad (8)$$

$$v_{b,e}^m|_H = M_b - m_{b,e}|_H \quad (9)$$

$$\Delta h_{n,z} = \begin{cases} h_{n,z} - h_{n,z-1}, & \text{if } h_{n,z} \leq h_n \\ 0, & \text{if } h_n \leq h_{n,z-1} \\ h_n - h_{n,z-1}; & \text{otherwise} \end{cases} \quad (10)$$

The objective function in Equation (11) deals with minimizing the overall cost of the contribution of storage devices. In the constraints of Equation (12), the parameter $\alpha_{b,e,n}^m[z]|_H d_{n,z}$ or $\Delta h_{n,z}$ is linearized in the form of z-segment virtual inertia related to the n th storage named $d_{n,z}$ or $\alpha_{b,n}^m[z]|_H d_{n,z}$. Hence, $\sum_{n \in \mathcal{E}, z \in \mathcal{E}_e} \alpha_{b,n}^m[z]|_H (d_{n,z} - \Delta h_{n,z})$ is the linear improvement of the considered indices, and $v_{b,e}^m|_H$ is the minimum improvement necessary for each index to observe its limits. Equation (13) represents the upper limit of the virtual inertia $d_{n,z}$ related to the z th part. Equations (14) and (15) state that none of the storage devices can produce virtual inertia between zero and \underline{H}_n . The $(z + 1)$ th part can establish

inertia only when the z th part proposes the whole inertia between $h_{n,z} - h_{n,z-1}$, and these constraints are given in Equations (16) and (17).

$$\min_{d,u}: c^T d \quad (11)$$

$$s. t: \text{ for } \forall b \in B, e \in \mathcal{E}, m \in M \quad (12)$$

$$\sum_{n \in N, z \in Z_n} \alpha_{b,e,n}^m[z]|_H (d_{n,z} - \Delta h_{n,z}) \geq v_{b,e}^m|_H \text{ for } \forall b \in B, e \in \mathcal{E}, z \in Z_n, n \in N \quad (13)$$

$$u_{n,z} \in \{0,1\} \quad (14)$$

$$d_{n,z} \leq u_{n,z}(h_{n,z} - h_{n,z-1}) \quad (15)$$

$$u_{n,0} h_{n,0} \leq d_{n,0} \quad (16)$$

$$u_{n,z+1}(h_{n,z} - h_{n,z-1}) \leq d_{n,z}, z \neq \bar{Z}_n \quad (17)$$

The linearized problem of the contribution of power plants has made it possible to implement iterative algorithms. Here, a two-step method to solve the problem is introduced. This method has two loops. The outer loop, denoted by s , updates the solution space and divides the solution space. The inner loop, denoted by k , will improve the required criteria when there is a violation in the RoCoF or the frequency nadir from the allowed limit. Equation (18) gives the relationship related to updating the outer loop.

$$v_{b,e}^{m(s,k)} = v_{b,e}^{m(s,k-1)} + \beta_{b,e}^{m(s,k)} (M_b - m_{b,e}|_H d^{*(s,k-1)}) \quad (18)$$

At the end of each outer loop s , the algorithm updates the center of the solution space of the problem $H^{(s+1)}$ using the obtained optimal solution $d^*|_{H(s,K_s)} = d^{*(s,K_s)}$. To guarantee the convergence of the proposed method, the coefficient $\alpha_n^{(s)} \in [0,1]$ is used to break the solution space. Again, the virtual inertial space of each storage device is divided into a new space. Therefore, the marginal profit and its related restrictions are as follows.

In other words, it can be said that in the planning stage, based on the base load, the on and off status of the power plants and their working point is determined from the previous day, taking into account the energy reserve, and based on that, a contract with the gas

supply company is drawn. Then, any difference that occurs on the current day will be determined by operation. In fact, in operation, on/off status is not an issue anymore, and the only goal is to change the generation capacity of power plants. Therefore, there is a possibility of some difference in the operating point of the power plants, their gas consumption, or measures such as load shedding, so that the load can be fully met and the security restrictions of the network are respected.

$$h_{n,0}^{(s+1)} = \max \left\{ \bar{H}_n, d_n^{*(s,K_s)} - \frac{\alpha_n^{(s)}}{2} (h_{n,\bar{Z}_n}^{(s)} - h_{n,0}^{(s)}) \right\} \quad (19)$$

$$h_{n,\bar{Z}_n}^{(s+1)} = \min \left\{ \bar{H}_n, d_n^{*(s,K_s)} + \frac{\alpha_n^{(s)}}{2} (h_{n,\bar{Z}_n}^{(s)} - h_{n,0}^{(s)}) \right\} \quad (20)$$

2.3.2. Sensitivity analysis of the problem

On the left side of Figure 8, the value in terms of related to bus 4 is shown for times $t = 1, 2,$ and 3 s. According to the obtained results, the changes in the frequency nadir have an almost linear relationship with the injected power ΔP . Hence, the sensitivity of the frequency nadir to the injected power at other points can be found from $\frac{\partial \Delta f_{b,e}^{\min}}{\partial \Delta p} = \frac{\partial \Delta f_{b,e}^{\min}}{\partial p}$. These changes are provided on the right side of Figure 8, where the nonlinear behavior of $\frac{\partial \Delta f_{b,e}^{\min}}{\partial p}$ at any moment is clearly observed. Similar results to Figure 8 are provided in Figure 9, which shows the RoCoF with respect to injected power. In this case, bus 1 (two nodes away from bus 69), bus 4 (two nodes away from bus 69), bus 43 (eleven nodes away from bus 69), and bus 17 (eleven nodes away from bus 69) are considered.

Figure 10 depicts the time-dependent changes of indices for bus 1 due to the injection of reactive power into bus 4.

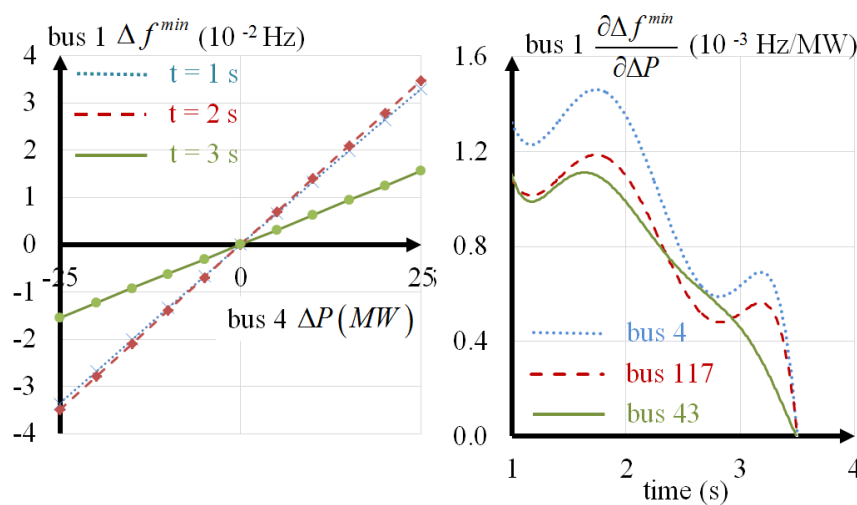


Figure 8. The minimum changes of frequency with respect to injected power.

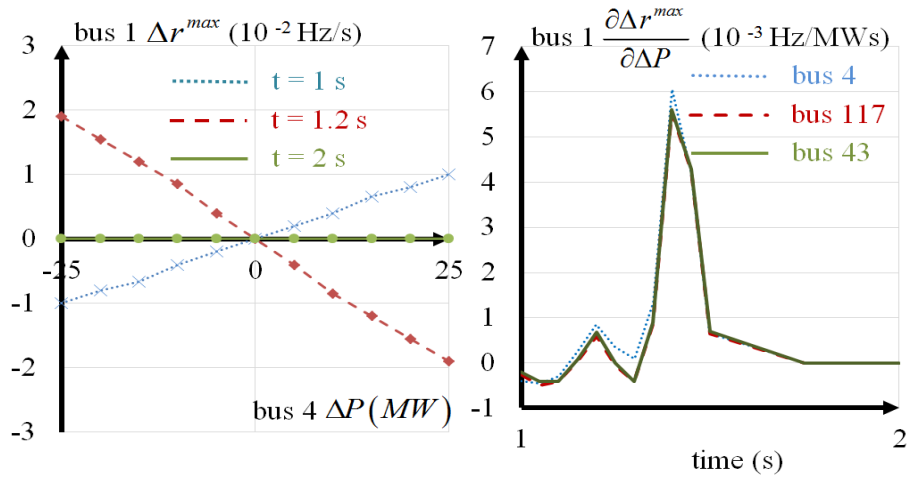


Figure 9. RoCoF in terms of injected active power.

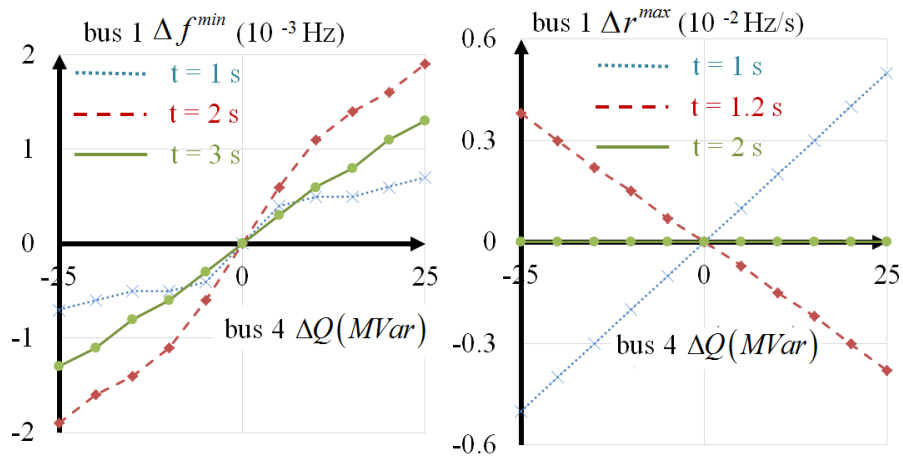


Figure 10. The change of time-dependent indices of bus 4 due to power injection into bus 4.

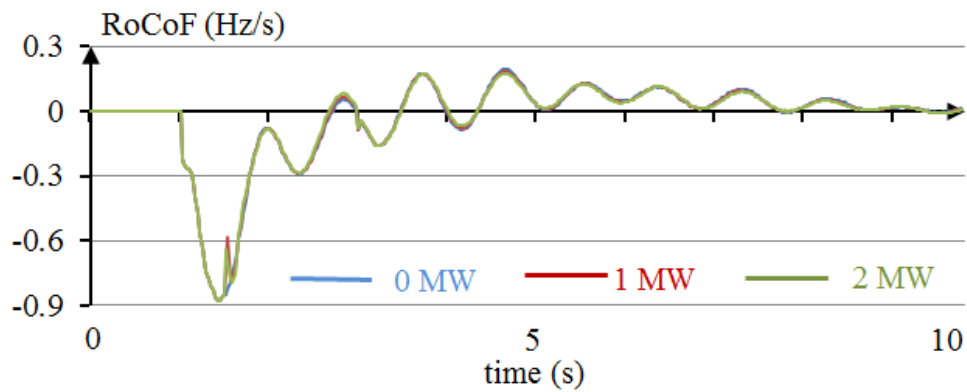


Figure 11. The RoCoF in bus 1 due to active power injection into bus 4.

The change of active power injected to bus 4 in time steps of 1.5 s with 0, 1, and 2 MW changes in the power value was analyzed. The graphs related to these changes are also shown in Figure 11. The results show that the output power of the storage devices has a small effect on the network frequency. Therefore, the estimation of each part can be estimated by reconstructing the frequency measurements in each bus.

3. Simulations and results analysis

In this paper, two networks have been examined. A three-bus network, which includes 4 generation units, 2 fast storage units, and 3 network load units. In this network, events usually occur in generation unit No. 4. The other network is the modified IEEE 118-bus network, which includes 8 fast storage units. The capacity of all storage units is considered equal to 15 MW. Also, the costs related to the energy supply of storage devices are different from each other. The energy storage capacity is also assumed to have no limit. There is a possibility of an event in four points of the network, where the generators located in bus 80 (the 389 MW unit), bus 100 (the 415 MW unit), bus 61 (the 386 MW unit), and bus 59 (the 433 MW unit), are among these cases. The permissible value of the frequency nadir and the maximum RoCoF are assumed to be 59.5 Hz and 0.5 Hz, respectively.

3.1. Case studies

In this paper, various study cases have been considered, each of which can represent a different aspect of simulation. These study cases are:

Case I: First, the effect of each technical parameter on the frequency response of the sample power system is investigated. A network with 10 traditional 120 MW units (1.2 p.u.) and variable inertia between 2.5 to 3.5 s (with steps of 0.1 s) and time constants $T_{i,1} = 0.5s$ $T_{i,2} = 2.5s$, $T_{i,3} = 5.5s$ has been considered. An event is assumed in which the load suddenly increases by 1 p.u. from the basic value of 10 p.u. and the amount of energy stored in the storage device is equal to zero. For all storage devices, we have $T_{fp} = 0.1s$ and $T_{sp} = 0.5s$. The purpose of this case is to somehow analyze the sensitivity of the model to the technical parameters of the problem.

Case II: In this case, the planning of the 3-bus network is carried out in such a way that it is necessary to solve the differential equations of the frequency swing in each case.

3.2. Simulation results

3.2.1. Case I

3.2.2.1. Impact of inertia of storage on frequency response

Figure 12 shows the effect of changing the inertia of energy storage on the frequency response of the power system. The output power of the storage device, the output power of the traditional power plants, and the frequency deviation in different values of the virtual inertia of the storage devices are shown. The higher the virtual inertia, the better the frequency response of the system. The frequency deviations or the distance between the frequency nadir and the nominal frequency are reduced and the intensity of the maximum RoCoF is also reduced. The deviation of the power balance of the network is answered with the simultaneous contribution of traditional power plants and energy storage. The more the inertia of grid storage devices increases, the contribution of storage devices to the power supply increases, and the share of traditional power plants

decreases. Therefore, higher values of virtual inertia require higher charging and discharging capacity of ESS.

3.2.1.2. Impact of the rated power of storage on frequency response

Figure 13 depicts the effect of rated power of energy storage on the frequency response of power systems. As can be seen, with the increase in charging and discharging capacity, the frequency response of the power system shows more improvement. Also, the contribution of ESS will increase.

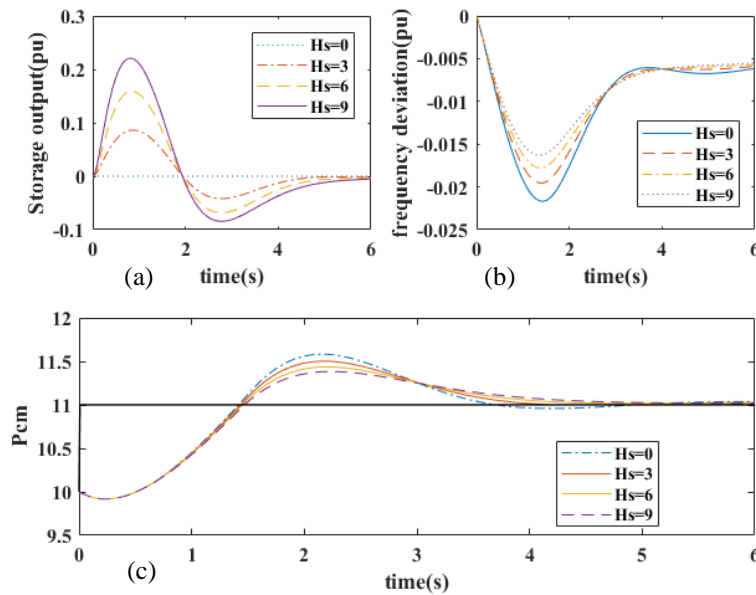


Figure 12. The effect of virtual inertia on the frequency response of the power system by considering the dynamics of the storage battery. (a) Frequency response (upper right), (b) storage output power (upper left), and (c) output power of traditional generators (bottom).

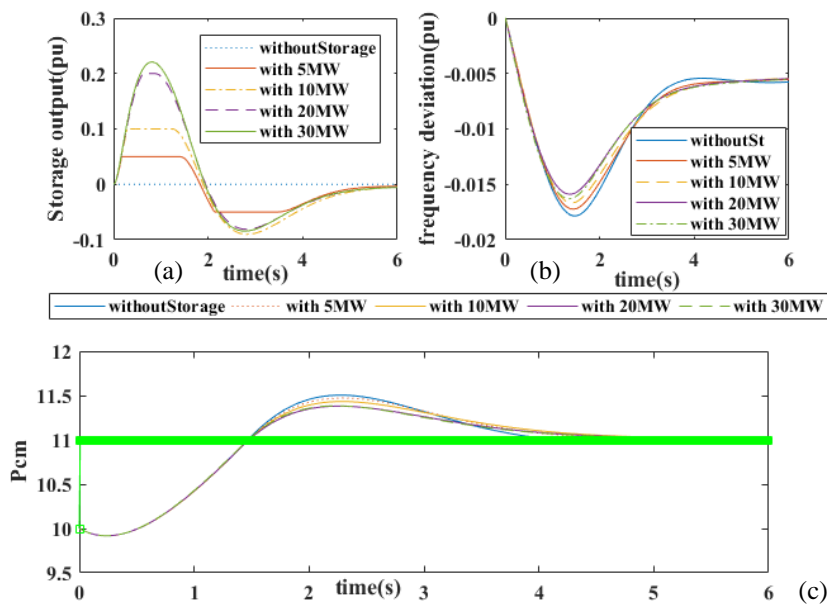


Figure 13. The effect of the rated power of the storage device on the frequency response of the network for $H_s = 9s$. (a) Frequency response (upper right), (b) storage output power (upper left), and (c) output power of traditional generators (bottom).

3.2.1.3. Impact of the rated power of storage on frequency response

Figure 14 shows the effect of the initial charge of the storage device on the frequency response. As it is known, the initial output values of the storage devices play a significant role in the behavior of the primary frequency response. The charging state of the storage devices helps to prevent the frequency drop and the discharging state of the storage devices brings a worse situation in terms of the frequency nadir compared to the state without the storage device. It should also be noted that the storage units with an initial output of -10 MW contribute to the inertial response exactly after the event, but the storage units with an initial output of 10 MW do this only after the frequency drops. These results seem reasonable. Storage devices usually have less free capacity to respond to frequency reduction.

3.2.2. Case II

Figure 15 shows the maximum RoCoF and the minimum frequency nadir of the network in the inertial space of storage batteries, which is divided into two categories: the possible space and the impossible (unacceptable) space. This space shows the importance of virtual inertial services and the non-linear relationship between selected parameters (such as the frequency nadir and RoCoF) with the virtual inertia of the network. To simultaneously meet the requirements of the RoCoF and the frequency nadir, it is necessary to find the intersection of the acceptable space of the two regions.

Table 1 lists some boundary points related to RoCoF and frequency nadir. As it is known, some of the solutions have provided only the constraint related to the frequency nadir, while others have provided that of the RoCoF, and some have met both constraints. The solution with the lowest allowed cost by observing both conditions is selected as the best solution to the optimization problem. In Table 1, red values are unacceptable while green ones are acceptable. The best solution obtained, which has the lowest cost among the allowed solutions, is marked with blue color.

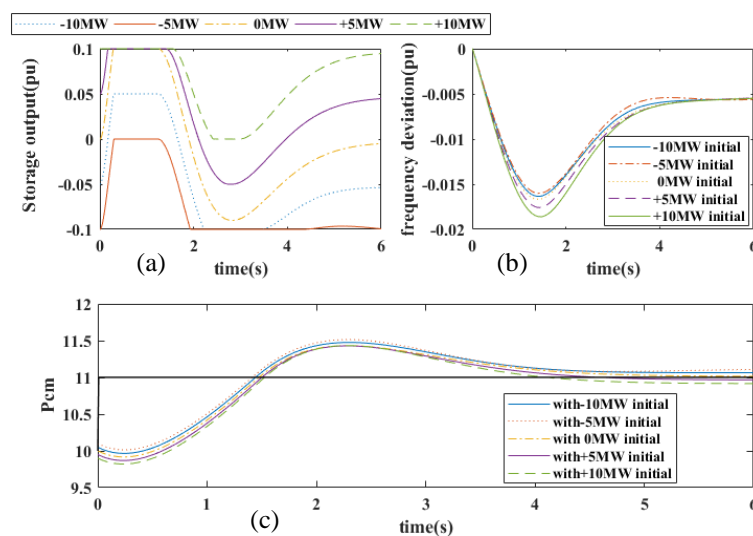


Figure 14. Investigating the effect of the initial charge level of the storage on the frequency response of the network for $H_s = 9s$. (a) Frequency response (upper right), (b) storage output power (upper left), and (c) output power of traditional generators (bottom).

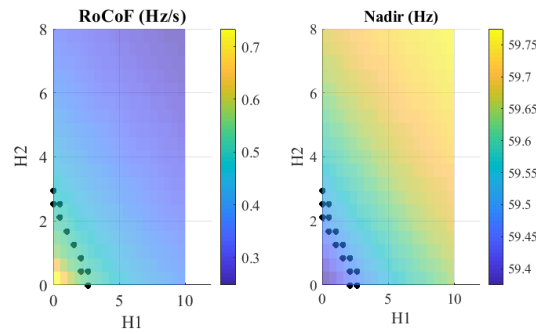


Figure 15. Maximum RoCoF (left) and frequency nadir (right) in different inertias of test network storages.

Table 1. Boundary points of constraints on frequency nadir and RoCoF.

H_1	H_2	RoCof	Frequency nadir	Cost (\$)
0	2.1053	0.5246	59.4823	421.0526
0	2.5263	0.5090	59.4997	505.2632
0	2.9474	0.4943	59.5159	589.4737
0.5263	1.6842	0.5206	59.4868	442.1053
0.5263	2.1053	0.5052	59.5038	526.3158
0.5263	2.5263	0.4907	59.5198	610.5263
1.0526	1.2632	0.5167	59.4911	463.1579
1.0526	1.6842	0.5015	59.5079	547.3684
1.5789	0.8421	0.5128	59.4954	484.2105
1.5789	1.2632	0.4979	59.5120	567.4211
2.1053	0	0.5246	59.4823	421.0526
2.1053	0.4211	0.5090	59.5159	589.4737
2.1053	0.8421	0.4943	59.5159	589.4737
2.6316	0	0.5052	59.5038	526.3158
2.6316	2.4211	0.4907	59.5198	610.5263

4. Conclusions

The formation of virtual inertia is one of the different methods of controlling ESS. By using power electronic converters connected to these sources, it is possible to contribute to the primary frequency response or inertial response if an event is detected. Since storage devices are highly capable of quickly increasing their power from the lowest value to the highest value, they can provide a significant improvement in the frequency response. In this paper, the storage parameters effective in the improvement of the frequency response of the network were investigated and the sensitivity analysis of the contribution of ESS to providing inertia for the initial frequency response was discussed. The effect of power capacity and energy storage, the amount of virtual inertia designed for it, etc. on the improvement of frequency response parameters such as RoCoF and frequency nadir were analyzed and investigated. Also, an optimization-based method for the optimal management of ESS was presented, which determined the best necessary inertia for each of the storages. These inertias were chosen in such a way that in addition to providing the boundary constraints of the problem, the amount of operating costs of the storage devices was minimized.

References

- [1] M. Sadeghi, and M. Abasi, "Optimal Placement and Sizing of Hybrid Superconducting Fault Current Limiter for Protection Coordination Restoration of the Distribution Networks in the Presence of Simultaneous Distributed Generation," *Electric Power Systems Research*, vol. 201, 107541, 2021.
- [2] Y. Yang, S. Bremner, C. Menictas, and M. Kay, "Battery Energy Storage System Size Determination in Renewable Energy Systems: A Review," *Renewable and Sustainable Energy Reviews*, vol. 91, pp. 109-125, 2018.
- [3] K. C. Divya, and J. Østergaard, "Battery Energy Storage Technology for Power Systems—An Overview," *Electric Power Systems Research*, vol. 79, no. 1, pp. 511-520, 2009.
- [4] S. Darvish Kermani, V. Davatgaran, A. Beigzadeh, and M. Joorabian, "Power Equations for Non-Detection Zone of Islanding Detection in Renewable-Energy-based Microgrids with Multiple Connection Points to Micro-Grids," *Journal of Green Energy Research and Innovation*, vol. 1, no. 1, pp. 55-65, 2024.
- [5] P. Du, "Design of New Primary Frequency Control Market for Hosting Frequency Response Reserve Offers from Both Generators and Loads," *Renewable Energy Integration for Bulk Power Systems: ERCOT and the Texas Interconnection*, pp. 137-175, 2023.
- [6] N. Riaz, L. Peltonen, et al., "Enhancing Primary Frequency Control in Microgrids through Self-Smoothing Photovoltaic Systems," *25th European Conference on Power Electronics and Applications (EPE'23 ECCE Europe)*, pp. 1-10, 2023.
- [7] X. Wei, Z. Jin, and G. Li, "Parameter Optimization for Temporary Primary Frequency Control of Wind Turbines Based on Analytical Derivation," *4th International Conference on Mechanical Instrumentation and Automation*, 2023.
- [8] A. H. Besheer, X. Liu, et al., "Overview on Fast Primary Frequency Adjustment Technology for Wind Power Future Low Inertia Systems," *Alexandria Engineering Journal*, vol. 78, no. 1, pp. 318-338, 2023.
- [9] T. Liu, P. Wang, et al., "Operation-Area-Constrained Adaptive Primary Frequency Support Strategy for Electric Vehicle Clusters," *Journal of Modern Power Systems and Clean Energy*, vol. 11, no. 6, pp. 1982-1994, 2023.
- [10] J. Li, R. Xiong, et al., "Design/Test of A Hybrid Energy Storage System for Primary Frequency Control using a Dynamic Droop Method in an Isolated Microgrid Power System," *Applied Energy*, vol. 201, no. 1, pp. 257-269, 2017.
- [11] T. R. Oliveira, W. W. A. G. Silva, and P. F. Donoso-Garcia, "Distributed Secondary Level Control for Energy Storage Management in DC Microgrids," *IEEE Transactions on Smart Grid*, vol. 8, no. 6, pp. 2597-2607, 2017.
- [12] Y. Wang, Y. Xu, et al., "Aggregated Energy Storage for Power System Frequency Control: A Finite-Time Consensus Approach," *IEEE Transactions on Power Systems*, vol. 10, no. 4, pp. 3675-3686, 2019.
- [13] J. Ebrahimi, and M. Abasi, "Design of a Power Management Strategy in Smart Distribution Networks with Wind Turbines and EV Charging Stations to Reduce Loss, Improve Voltage Profile, and Increase Hosting Capacity of the Network," *Journal of Green Energy Research and Innovation*, vol. 1, no. 1, pp. 1-15, 2024.
- [14] S. Sharma, S. H. Huang, and N. D. R. Sarma, "System Inertia Frequency Response Estimation and Impact of Renewable Resources in ERCOT Interconnection," *IEEE Power and Energy Society General Meeting*, pp.1-6, 2011.
- [15] L. Sigrist, "A UFLS Scheme for Small Isolated Power Systems Using Rate-Of-Change of Frequency," *IEEE Transactions on Power Systems*, vol. 30, no. 4, pp. 2192-2193, 2015.
- [16] Y. Wen, W. Li, G. Huang, and X. Liu, "Frequency Dynamics Constrained Unit Commitment with Battery Energy Storage," *IEEE Transactions on Power Systems*, vol. 31, no. 6, pp. 5115-5125, 2016.
- [17] A. Ahmadi, A. E. Nezhad, and B. Hredzak, "Security-Constrained Unit Commitment in Presence of Lithium-Ion Battery Storage Units using Information-Gap Decision Theory," *IEEE Transactions on Industrial Informatics*, vol. 15, no. 1, pp. 148-157, 2019.

- [18] M. Carrion, Y. Dvorkin, and H. Pandzic, "Primary Frequency Response in Capacity Expansion with Energy Storage," *IEEE Transactions on Power Systems*, vol. 33, no. 2, pp. 1824-1835, 2018.
- [19] T. Xu, W. Jang, and T. Overbye, "Commitment of Fast-Responding Storage Devices to Mimic Inertia for the Enhancement of Primary Frequency Response," *IEEE Transactions on Power Systems*, vol. 33, no. 2, pp. 1219-1230, 2018.
- [20] T. Chakraborty, D. Watson, and M. Rodgers, "Automatic Generation Control Using an Energy Storage System in a Wind Park," *IEEE Transactions on Power Systems*, vol. 33, no. 1, pp. 198-205, 2018.
- [21] G. C. Gisse, P. E. Dodds, and J. Radcliffe, "Market and Regulatory Barriers to Electrical Energy Storage Innovation," *Renewable and Sustainable Energy Reviews*, vol. 82, pp. 781-790, 2018.
- [22] J. Cao, D. Wenjuan, W. Haifeng, and M. McCulloch, "Optimal Sizing and Control Strategies for Hybrid Storage System as Limited by Grid Frequency Deviations," *IEEE Transactions on Power Systems*, vol. 33, no. 5, pp. 5486-5495, 2018.
- [23] Y. Wen, W. Li, G. Huang, and X. Liu, "Frequency Dynamics Constrained Unit Commitment with Battery Energy Storage," *IEEE Transactions on Power Systems*, vol. 31, no. 6, pp. 5115-5125, 2016.
- [24] M. Ramirez, R. Castellanos, G. Calderon, and O. Malik, "Placement and Sizing of Battery Energy Storage for Primary Frequency Control in an Isolated Section of the Mexican Power System," *Electric Power Systems Research*, vol. 160, pp. 142-150, 2018.
- [25] B. Lian, A. Sims, D. Yu, C. Wang, and R. W. Dunn, "Optimizing Lifepo4 Battery Energy Storage Systems for Frequency Response in the UK System," *IEEE Transactions on Sustainable Energy*, vol. 8, no. 1, pp. 385-394, 2016.
- [26] S. Pulendran, and J. E. Tate, "Energy Storage System Control for Prevention of Transient Under-Frequency Load Shedding," *IEEE Transactions on Smart Grid*, vol. 8, no. 2, pp. 927-936, 2017.
- [27] G. He, Q. Chen, C. Kang, Q. Xia, and K. Poolla, "Cooperation of Wind Power and Battery Storage to Provide Frequency Regulation in Power Markets," *IEEE Transactions on Power Systems*, vol. 32, no. 5, pp. 3559-3568, 2017.
- [28] M. Abasi, M. Joorabian, A. Saffarian, and S. G. Seifossadat, "A Comprehensive Review of Various Fault Location Methods for Transmission Lines Compensated by FACTS devices and Series Capacitors," *Journal of Operation and Automation in Power Engineering*, vol. 9, no. 3, pp. 213-225, 2021.
- [29] M. F. Arani, and Y. A. R. I. Mohamed, "Cooperative Control of Wind Power Generator and Electric Vehicles for Microgrid Primary Frequency Regulation," *IEEE Transactions on Smart Grid*, vol. 9, no. 6, pp. 5677-5686, 2018.
- [30] S. Izadkhast, P. Garcia-Gonzalez, P. Frias, and P. Bauer, "Design of Plug-In Electric Vehicle's Frequency-Droop Controller for Primary Frequency Control and Performance Assessment," *IEEE Transactions on Power Systems*, vol. 32, no. 6, pp. 4241-4254, 2017.
- [31] M. Abasi, M. F. Nezhadaneini, M. Karimi, and N. Yousefi, "A Novel Metaheuristic Approach to Solve Unit Commitment Problem in the Presence of Wind Farms," *Rev Roumaine des Sciences Techniques-Series Electrotechnique et Energetique*, vol. 60, no. 3, pp. 253-262, 2015.

Declaration of Competing Interest

The authors declare that they have no known competing financial interests or personal relationships that could have appeared to influence the work reported in this paper. The ethical issues, including plagiarism, informed consent, misconduct, data fabrication and/or falsification, double publication and/or submission, redundancy, have been completely observed by the authors.

Credit Authorship Contribution Statement

Moaiaad Mohseni: Conceptualization, Data curation, Formal analysis, Methodology, Validation, Roles/Writing-original draft. **Alireza Niknam Kumle:** Conceptualization, Data curation, Formal analysis, Methodology, Software, Validation. **Rezvan Keshavarzpour:** Methodology, Software, Validation.

Bibliography



Moaiaad Mohseni was born in Kuwait. He received his B.SC Degree in Electrical Engineering, Kazeroon Branch, Islamic Azad University, Kazeroon, Iran in 2001, and his M.S. and Ph.D. degrees in Electrical Engineering from Dezful Branch, Islamic Azad University, Dezful, Iran, in 2011 and 2021, respectively. His Research Include Power Market and Smart Grid and renewable energy systems.



Alireza Niknam Kumle born in Iran in 1989, obtained a Ph.D. in Electrical Power Engineering from Shahid Chamran University of Ahvaz in 2021. With over 60 published papers and 10 authored books, he has completed 11 industrial research projects and holds a power systems patent. Recognized as the top researcher in Khuzestan province in 2021, he received four titles from the National Elite Foundation from 2021 to 2023. Currently an Assistant Professor at Arak University's Electrical Engineering Department, Kumle focuses on fault analysis, reactive power control, power quality improvement, and FACTS devices in HVAC and HVDC transmission lines.



Rezvan Keshavarzpour was born in Iran in 1990. She received her bachelor's and master's degrees in Electronics Engineering and Electrical Engineering (Power Systems) from Islamic Azad Universities of Shooshtar and Ahvaz branches, Iran, in 2014 and 2019, respectively. She is now employed at National Iranian South Oil Company (NISOC), Ahvaz, Iran. Her specialized interests include evaluation and improvement of power quality of power systems, operation of power systems, and protection of power systems.